



A Novel Adaptive Multiple-Access Scheme for Wireless Chip Area Network in the Smart Grid System

Xin-Yue Luo, Hao Gao, and Xue-Hua Li^(✉)

School of Information and Communication Engineering,
Beijing Information Science and Technology University, Beijing, China
lixuehua@bistu.edu.com.cn

Abstract. The design and construction of the smart grid system in 5G ultra-dense network needs to be effectively integrated with the mobile communication technology. Wireless chip area network (WCAN), as an application of the smart grid, has promising research potential. Focusing on the issue of multi-user network communication, this paper proposes an adaptive time-hopping pulse position modulation (TH-PPM) multiple access scheme that is applicable to WCAN. Combined with the specific applications of WCAN, the wireless channel characteristics of intra/inter chip communication are investigated, the bit error rate (BER) performance of the THPPM multiple-access system is analyzed; then, based on the aforementioned results, an adaptive TH-PPM multiple-access distribution mechanism is proposed and an intelligent transmission mechanism is designed to appropriately select the monopulse signal-to-noise ratio of the intra/inter chip, BER, and transmission rate in WCAN. Finally, the performance is analyzed through simulation and is also compared with the fixed multiple-access technology. The results show that on the premise of ensuring wireless interconnection quality of service of the intra/inter chip, this scheme can allocate system rate and power resource properly, strengthen transmission performance, and address the limitations of fixed multiple-access technology. The findings presented in this paper provide a reference for multi-user multiple-access communication with large capacity.

Keywords: Smart grid · 5G technology · Chip wireless interconnection · Wireless chip area network · Adaptive TH-PPM

1 Introduction

With the increasing demand for electricity, the load on the power grid construction has also increased. The traditional grid operation mode has become increasingly incapable [1]. Therefore, the demand for smart grids with high speed, high integration and good real-time performance is on the rise. In the smart grid,

mobile communication technologies are needed to assist the completion in order to acquire, analyze and process the grid data better, providing reliable power protection for the stable development of society [2].

In the future, mobile communication will occur not only between persons, but will also develop into intelligent interconnections between persons and things, among sensor devices, among intelligent chips, from machine to machine (M2M), and from device to device (D2D), all of which will account for more than 70% of mobile data service. The research on 5G technologies currently focuses on dense networks, device-to-device technology, new-type network architecture, high-band communication, new-type multiple antenna multiple distribution transmission technologies, for the purpose of increasing 4G transmission rate 101000 times, decreasing network delay 510 times and realizing wireless communication with low power consumption and high spectral efficiency [3]. In recent years, the remarkable development of intra/inter-chip wireless intercommunication technology based on high-band UWB and 60 GHz millimeter waves [4–9] has provided technical support to achieve the aforementioned goal as well as to provide a new application situation for 5G super-dense network, namely, wireless chip area network (WCAN). This development can achieve high-speed interconnection and efficient network organization [7–12] of inner integrated circuits, intra/inter chips in PCB, multiprocessor cores in system-on-chip (SoC) circuits, intelligent appliances, and mobile terminals. However, most current research on-chip wireless interconnection technology focuses on point-to-point wireless communication of single users and the transmission data are relatively limited. The application of WCAN is definitely the mode of communication with a large amount of data in the context of multiple users; multi-user interference and inter-symbol interference are the problems that must be considered. Simple modulation schemes such as OOK [4] and BPSK [5–7] cannot meet the requirements of actual application while the OFDM scheme [8] increases the design complexity. Although multiple-access technologies such as TDMA, CDMA, DSBPSK, and TH-PPM are adopted to achieve multiple Intra/inter-chip wireless interconnection [13–17], all of these are at the level of circuit design and BER performance is not analyzed. Meanwhile, the fixed multiple-access distribution scheme adopted wastes the resources when users are few and cannot meet the requirements of system performance when users are many. As a result, a more effective multiple-access technology is needed to raise the transmission performance of the system. An adaptive multiple-access scheme applicable to specific applications of WCAN should be investigated.

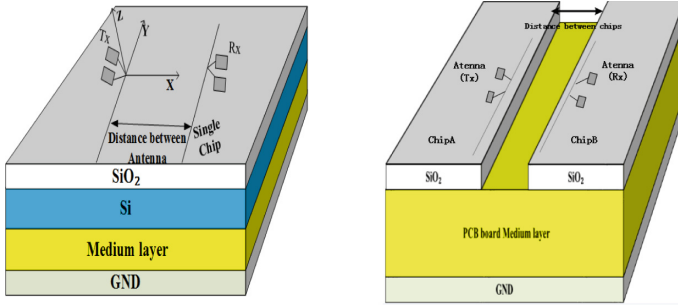
This paper is organized as follows. The research background is introduced in Sect. 1. TH-PPM multiple-access performance in WCAN is analyzed in Sect. 2. An adaptive multiple-address design scheme based on TH-PPM is proposed in Sect. 3. The advantages of the proposed scheme compared with those of the traditional fixed multiple-access mechanism are presented in Sect. 4. The research findings are summarized in Sect. 5.

2 Performance Analysis of TH-PPM Multiple-Access in WCAN

In the multiple-access technology based on high-band IR-UWB and 60 GHz pulse radio, TH-PPM technology is comparatively mature. TH-PPM separates pulse repetition period into several time slots by taking advantage of the feature of the minimum duty cycle of UWB pulse signal and combining it with TDMA and CDMA technologies. TH-PPM distinguishes users by different pseudo-random time-hopping codes, and controls pulse position by using data symbols. Compared with DS-BPSK [15], TH-PPM does not need to control the pulse amplitude and polarity requires lower sensitivity with regard to near-far effect and reduces the difficulty of power control, which easily achieves high-speed communication of multiple I/O devices or multiple chips by lower complexity in a shorter distance. In the multichannel context, problems related to crosstalk and resource allocation can be solved by setting the matched multiple-access methods in the layer of MAC. In terms of reducing system complexity and power consumption, the TH-PPM multiple-access modulation technology is suitable for intra/inter-chip wireless interconnection systems. The TH-PPM multiple access technology is adopted in references [16] and [17] to achieve multi-user data-parallel transmission in intra/inter-chip wireless interconnection systems; the circuit design scheme is proposed, but the BER performance is not analyzed. In this section of the current paper, the intra/inter-chip physical channel characteristics, multi-user interference characteristics of intra/inter-chip adopting TH-PPM, noise source, and BER performance are analyzed.

2.1 Intra/Inter-chip Physical Channel Characteristics

The characteristics of a channel, as an indispensable part of the system, has a significant effect on the system performance and design. In the current WCAN networking schemes, intra/inter-chip closely adopts multi-hop self-organizing communications. Electromagnetic signals are line-of-sight transmissions in adjacent processor cores or chips. A simple intra-chip wireless interconnection model and an inter-chip wireless interconnection model are separately shown in Figs. 1(a) and 1(b) [18]. The transmission distance of the intra/inter-chip wireless channel is usually at the level of cm or even mm, and the energy of surface wave accounts for more than 80% of the total energy. The multipath delay is negligible, so the channel can be considered as a Rice channel. Under the ideal medium, the advantage of the surface wave becomes highly obvious, and the Rice factor K value tends to infinity at that moment, so that the intra/inter-chip the channel can be approximately considered as a Gaussian channel. For the sake of theoretical analysis, the Gaussian channel is taken as a channel in this research model and the WCAN composed of chip wireless interconnection in the PCB is the research subject.



(a) Intra-chip wireless interconnection model (b) Inter-chip wireless interconnection model

Fig. 1. wireless interconnection model

2.2 Analysis of Multi-user Interference Characteristics in System

In WCAN, the TH-PPM signal of user can be expressed as [16,17,19]:

$$s^{(k)}(t) = \sum_{j=-\infty}^{\infty} \sqrt{E_w} p_{tr} \left(t - jT_f - c_j^{(k)} T_c - \delta d_{[j/N_s]}^{(k)} \right) \tag{1}$$

$p_{tr}(t)$ is an energy normalized monocycle pulse waveform, that is, $\int_{-\infty}^{\infty} |p_{tr}|^2 dt = 1$. Its pulse width is T_p , its chip duration is T_c , and $T_p \leq T_c$. $N_h = T_f/T_c$ is the upper limit of maximum value of time-hopping code, T_f is the frame length, $0 \leq c_j^{(k)} < N_h$ is the pseudo-random time-hopping code sequence of user K (user address code), $[x]$ represents rounding to x . $d_j^{(k)} \in [0, 1]$ is a binary value of the j th pulse transmission of user K . N_s is pulse number of per bit; average pulse repetition period of per bit can be expressed as $T_s = N_s T_f$, so the information bit rate is $R_b = (N_s T_f)^{-1} = (N_s N_h T_c)^{-1}$. δ represents PPM deviation, E_w indicates normalized monocycle pulse waveform energy, and $E_b = N_s E_w$ is information energy per bit. The mentioned relationship is shown by Gaussian pulse waveform in Fig. 2.

To analyze the transmission performance of users in WCAN, the following hypotheses are set:

1. users conduct wireless communications in the system; 0 and 1 with equal probability occurrence and independent identical distribution in the data sequence are produced by all users.
2. Pseudo-noise (PN) code adopted by each user is a gold code, which occurs at random and is mutually independent and equiprobable.
3. For the purpose of improved system flexibility, the antenna gain of receiver and transmitter is 0 dBi.
4. Each user adopts coherent reception, and its specific PN code is known when reception occurs and the soft decision is implemented after detection.

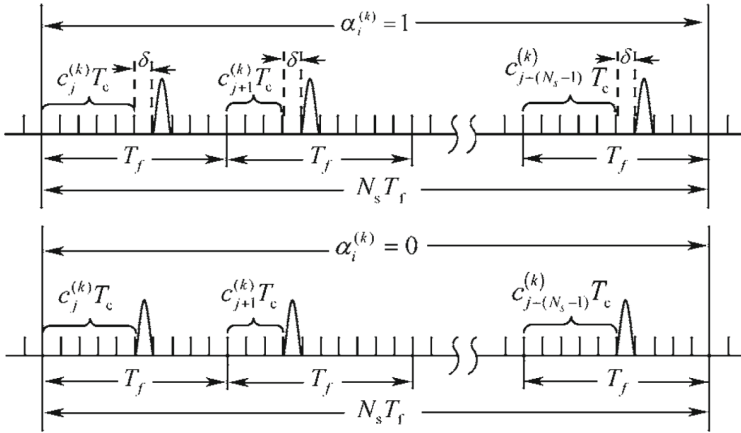


Fig. 2. TH-PPM modulation waveform

5. The system is an asynchronous self-organizing network, but it is based on the assumption that adopting coherent detection, reference receiver, and the corresponding transmitter is totally synchronous.
6. All users can spread ideally and freely without multi-path influence.

Channel impulsion response without multi-path of k th user and its reference receiver is the function of path loss A_k and transmission time delay τ_k . Transmission time delay is mutually independent and it obeys uniform distribution in $[0, T_c)$. Then, in the same environment condition when k users implement transmitting, the total signal received by the reference receiver is

$$\begin{aligned}
 r(t) &= \sum_{k=0}^{N_u-1} A_k s_{rec}^{(k)}(t - \tau_k) + n(t) \\
 &= A_0 s_{rec}^{(0)}(t - \tau_0) + \sum_{k=1}^{N_u-1} A_k s_{rec}^{(k)}(t - \tau_k) + n(t)
 \end{aligned}
 \tag{2}$$

In decision, because of coherent detection, the signals from the other users are considered as multi-user inference. Let user 0 be the main receiving signal, and then $S_{rec}^{(0)}(t - \tau_0)$ in Eq. (2) is a useful signal; $\sum_{k=1}^{N_u-1} A_k s_{rec}^{(k)}(t - \tau_k)$ is the multi-user inference signal, where $s_{rec}^{(k)}(t)$ is the receiving signal of user k , and as a result of transient characteristics of high-frequency pulse signal, the waveform of should be the second-order differential of transmitting signal $p^{(k)}(t)$. $n(t)$ indicates two types of noise, namely, thermal and switching, that mainly occur in the intra/inter-chip wireless interconnection system [7]. The value of switching noise is usually 10 dB less than that of thermal noise, and its bilateral power spectrum density is $N_0/2$. According to the calculation method of noise power

spectrum in [7], the regulated receiving antenna temperature of the intra/inter-chip wireless interconnection system is $T_{ant} = 330\text{K}$ and the regulated noise index of the receiver is $F_r = 10\text{ dB}$; thus, thermal noise power spectrum density can be calculated as -163.92 dBm/Hz . Now, the total noise power spectrum density is $N_0 = N_{\text{thermal}} + N_{\text{switching}} = -163.504\text{ dBm/Hz}$, and this value is used in the following simulation analysis.

When user 0 receiver performs the detection, correlation masks need to be provided as follows:

$$m^{(0)}(t) = \sum_{j=0}^{N_s-1} v^{(0)} \left(t - jT_f - c_j^{(0)}T_c \right) \tag{3}$$

$$v^{(0)}(t) = p_{rec}^{(0)}(t) - p_{rec}^{(0)}(t - \delta) \tag{4}$$

Receiving signal $r(t)$ is multiplied by $m^{(0)}(t - \tau_0)$ and the calculating output is

$$Z^{(0)} = \int_0^{T_b} r(t)m^{(0)}(t - \tau_0) dt \tag{5}$$

Place Eqs. (1) (2) (3) (4) in Eq. (5) as follows:

$$Z^{(0)} = Z_0 + Z_{mui} + Z_n \tag{6}$$

In the equation, Z_0 is useful user correlation detection output, Z_{mui} is multi-user interference, and Z_n is Gaussian noise correlation output. According to reference [20]

$$\begin{aligned} Z_0 &= N_s \int_{-\infty}^{\infty} A_0 \sqrt{E_w} s_{rec}^{(0)}(t - \tau_0) m^{(0)}(t - \tau_0) dt \\ &= \begin{cases} +A_0 N_s \sqrt{E_w} [1 - r(\delta)] & d_j^{(0)} = 0 \\ -A_0 N_s \sqrt{E_w} [1 - r(\delta)] & d_j^{(0)} = 1 \end{cases} \end{aligned} \tag{7}$$

$$\begin{aligned} Z_n &= \sum_{k=1}^{N_u} \sum_{j=0}^{N_s-1} \int_{\tau_0 + jT_f}^{\tau_0 + (j+1)T_f} n(t) [p_{rec}^{(0)}(t - jT_f - c_j^{(0)}T - \tau_0) \\ &\quad - p_{rec}^{(0)}(t - jT_f - c_j^{(0)}T - \delta - \tau_0)] dt \end{aligned} \tag{8}$$

$$\begin{aligned} Z_{mui} &= \sum_{k=1}^{N_u} \sum_{j=1}^{N_s-1} \int_{\tau_0 + jT_f}^{\tau_0 + (j+1)T_f} A_k s_{rec}^{(k)}(t - \tau_k) [p_{rec}^{(0)}(t - jT_f - c_j^{(0)}T - \tau_0) \\ &\quad - p_{rec}^{(0)}(t - jT_f - c_j^{(0)}T - \delta - \tau_0)] dt \end{aligned} \tag{9}$$

2.3 Performance Analysis of System Signal-to-Interference and Noise Ratio and BER

Since each user suffers the same degree of interference in WCAN, the transmission performance of the entire network can be measured according to the BER performance of signals received by each user. BER is the function of signal-to-interference and noise ratio (SINR), and determining the value of SINR in WCAN is extremely important. SINR and BER are analyzed when each chip conducts wireless communication in WCAN. Based on the correlation detection equations illustrated in Sect. 2.2, the sum of useful energy of N_s pulses that compose a 1 bit output in the receiver is

$$E_b = E(Z_0^2) = E_w^{(0)} A_0^2 N_s^2 [1 - r(\delta)]^2 \tag{10}$$

For system flexibility, let the antenna gain of receiver and transmitter G_{tx} and G_{rx} be 0dBi. If the distance between the transmitting antenna and the receiving antenna is d , then the wavelength of the antenna is λ , and path loss A_0^2 can be obtained according to the transmission loss model of space free wave as follows:

$$A_o^2 = G_{tx} G_{rx} \left(\frac{\lambda}{4\pi d} \right)^2 \tag{11}$$

The variance of output noise of the receiver is

$$\sigma_n^2 = E(Z_n^2) = N_s N_0 [1 - r(\delta)] \tag{12}$$

Reference [21] uses probability statistics to get multi-user interference variance, and combining with Eq. (9), multi-user interference variance in 1 bit is

$$\sigma_{mii}^2 = E(Z_{mi}^2) = \frac{T_p}{T_f} N_s [1 - r(\delta)]^2 \sum_{k=1}^{N_i-1} A_k^2 E_w^{(k)} \tag{13}$$

Since Z_{mui} and Z_n obey Gaussian distribution with the mean value being 0 and the variances being σ_{mui}^2 and σ_n^2 separately, the SINR of the system is

$$\begin{aligned} SMR &= \frac{E_b}{\sigma_{mii}^2 + \sigma_n^2} \\ &= \frac{E_w^{(0)} \hat{f}^2 N_s^2 [1 - r(\delta)]}{\frac{T_p}{T_f} N_s [1 - r(\delta)]^2 \sum_{k=1}^{N-1} A^2 E_w^{(k)} + N_s N_0 [1 - r(\delta)]} \end{aligned} \tag{14}$$

To decrease intersymbol interference and maintain good transmission performance, quadrature PPM modulation is used in WCAN-PCB. When $T_c \geq 2T_p$, let $T_c = \beta T_p$, then $1/\beta$ expresses the duty cycle of pulse and $\beta \geq 2$, and now the coherent coefficient is $r(\delta) = 0$. Meanwhile, to facilitate analysis, we suppose

that path loss A_k is the same in the transmission of each link among chips, and if $SNR = \frac{E_w A_0^2}{N_0}$ expresses the SNR of unit pulse, then Eq. (14) is simplified as

$$SINR = \frac{N_s}{\frac{T_p(N_u-1)}{T_c N_h} + \frac{N_0}{E_w A_0^2}} = \frac{N_s}{\frac{N_u-1}{\beta N_h} + \frac{1}{SNR}} \quad (15)$$

According to the relationship between SINR and BER, and based on TH-PPM multiple-access modulation technology, the BER formula of a multiple inter-chip wireless interconnection system is expressed as

$$BER = \frac{1}{2} \operatorname{erfc} \left(\sqrt{\frac{SINR}{2}} \right) = \frac{1}{2} \operatorname{erfc} \left(\sqrt{\frac{N_s}{\frac{2(N_u-1)}{\beta N_h} + \frac{2}{SNR}}} \right) \quad (16)$$

From Eqs.(15) and (16), we find that the values of multi-user SINR and BER in WCAN-PCB are correlated with β (reciprocal value of pulse duty cycle, which depends on the values of T_p and T_c , generally fixed value), N_u (number of users), N_s (number of pulses of each bit), N_h (upper limit of maximum value of time-hopping code), SNR (signal-to-noise ratio of unit pulse), among which the values of N_s and N_h decide the bit transmission rate R_b of users, and SNR and N_s decide the transmitting power of the system.

3 Design of Adaptive TH-PPM Multiple-Access Distribution Scheme in WCAN

In WCAN, because of random access of chips to a certain extent, the network topology structure shows dynamic change, and in the system, noise interference and channel characteristics change randomly. In the wireless communication system, link adaptive technology is used to solve the problems of signal loss and transmission quality decrease caused by a random chance of the channel with multiple users, in which adaptive modulation coding technology and adaptive multiple-access resource distribution technology are used widely. However, adaptive modulation coding technology requires various types of modulation and coding circuits in chips, which is unacceptable to the chip wireless interconnection system because the complex system has strict cost and design requirements. Comparatively, adaptive multiple-access resource distribution technology does not need an additional modulation coding circuit, and automatic distribution of system resources is achieved by real-time adjustment of rate and power, and in this way, this technology is superior to the former in terms of design complexity and cost. For example, a scheme of self-adaptive adjusting code length dynamically proposed in references [22] and [23] can guarantee a higher transmission rate of nodes regardless of power limitation. The TH-PPM multiple-access scheme specific to the WCAN system proposed in [16] and [17] solves multi-user interference to a certain extent, but the scheme adopts a fixed multiple-access mechanism (FMAM) that cannot meet the requirements of changeable

QoS, that is, FMAM may waste considerable system resources when the channel environment is good while communication may not be guaranteed when the channel environment is bad. In this section, an adaptive multiple-access mechanism (AMAM) based on TH-PPM is proposed, which can alter the transmission rate or transmitting power in real-time and select the best resource distribution scheme automatically according to the channel environment; under the demand of QoS, the mechanism can enable the entire system to maintain high communication capacity and low power. Weighing quality, rate, and power of communication is the core of an adaptive algorithm. The adaptive multiple-access distribution scheme in WCAN is shown in Fig. 3.

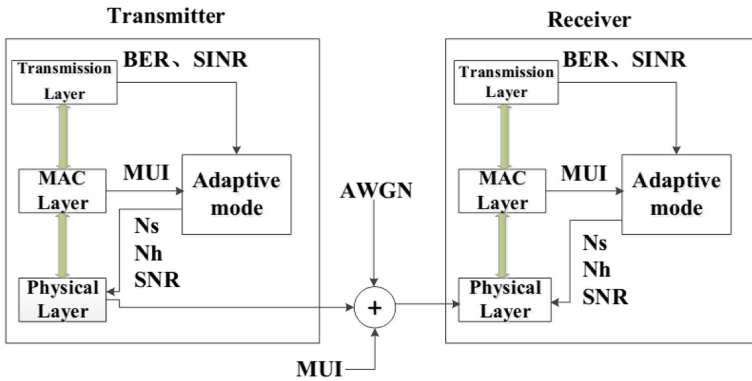


Fig. 3. Adaptive multiple-access distribution scheme in WCAN

In Fig. 3, because N_u and β are known, the BER performance of the system is related to the selection of N_s , N_h , and SNR, and as a result, according to MUI and thermal noise interference originating from various N_u , the adaptive mode chooses the best multiple-access distribution scheme, allowing the entire system to remain relatively stable. The selection process is shown as follows:

- 1) To guarantee the stability of the system, the value of BER cannot exceed the regulated threshold of QoS, as shown in Table 1, so N_s , N_h , and SNR must meet Eq. (17). From the perspective of elevating resource utilization in maximum, the SINR value of the best multiple-access distribution scheme should be a threshold that meets the regulation of QoS. At this point, if N_s and N_h are confirmed, then the corresponding SNR is obtained.

Table 1. BER upper limit and corresponding SINR threshold required by QoS.

BER level	10^{-4}	10^{-5}	10^{-6}	10^{-7}	10^{-8}	10^{-9}
Required SINR	13.8311	18.1893	22.5950	27.0331	31.4946	35.9737

$$SNR = \frac{N_s}{\frac{N_u-1}{\beta N_h} + \frac{1}{SNR}} \geq SNR_{\text{trashdd}} \tag{17}$$

2) When the system meets the requirements of QoS, to enable the system to maintain lower power consumption, the SNR threshold of each user should be defined as follows:

$$SNR = \frac{1}{\frac{N_s}{SNR_{\text{threshold}}} - \frac{N_u-1}{N_h\beta}} \leq SNR_{\text{threshold}} \tag{18}$$

3) To guarantee high-speed transmission for each user in the system, when steps 1) and 2) are finished, the smaller value of $N_s \times N_h$ needs to be selected. The following equation should be satisfied:

$$MIN [N_s \times N_h] \leq N_s \times N_h \leq MIN [N_s \times N_h] + 3 \tag{19}$$

4) After step 1), steps 2) and 3) are completed, and the combination value of N_s and N_h has to be selected ultimately. If the value of N_s is significantly larger, the pulse transmitted by each bit increases, which then increases the total transmitting power; if the value of N_h is significantly larger, the design complexity of the encoder increases. To weigh the values of N_s and N_h and decrease the design complexity, if the values of $N_s \times N_h$ in several combinations are close, then the combination with the largest value of $N_h^{N_s}$ is selected; at this point, the number of PN codes distributed by the system is the largest, which can reduce intersymbol interference effectively.

The combination of N_s, N_h and SNR selected through the aforementioned algorithm is the best multiple-access distribution scheme, and furthermore, the corresponding bit rate R_b of the signal user and the average power P_{ave} are obtained from the following equations:

$$R_b = \frac{1}{N_s N_h T_c} \tag{20}$$

$$P_{\text{ave}} = \frac{N_s \times SNR \times N_0}{T_c} \tag{21}$$

4 Performance Simulation and Analysis

Based on the adaptive multiple-access distribution scheme proposed in the previous section, the change tendency of information rate R_b and average power P_{ave} of each user in the system following the number of access users N_u is comparatively analyzed through simulation under the AMAM and FMAM schemes separately.

The simulation parameters are set as follows: $N_0 = -163.504$ dBm/Hz, $SNR_{\text{threshold}} = 15$ dB, $f_c = 10$ GHz, $\beta = 8$, $BER = 10^{-4}$. FMAM adopts a fixed parameter setting, while AMAM selects the optimal multiple-access distribution scheme that matches the number of access users N_u in real time according to the change of number.

4.1 Relationship Between Number of Users N_u and Information Rate R_b

The value of R_b reflects the speed of data transmission of the intra/inter chip. Figure 4 shows the relationship between N_u and R_b under the AMAM and FMAM schemes. R_{bi} expresses the rate value of i th FMAM for a single user, and the simulation results show that as long as the values of N_{si} and N_{hi} are defined, the value of R_{bi} is invariable and is inversely proportional to the value of $N_{si} \times N_{ki}$ and unrelated to the value of N_u . Meanwhile, each FMAM corresponds to one $N_{u_{max\ i}}$ that means the maximum number of users supported by the communication system with reliable quality. Once the number of user access has exceeded the maximum, the communication quality of the system is lost. For example, FMAM with [SNR = 15 dB, NsNh (3,4)], although $R_{N1} = 833$ Mbps has a higher transmission rate, only when the number of users is fewer than six can the communication quality be guaranteed; thus, this FMAM does not apply to the system with many users. However, FMAM with [SNR = 15 dB, NsNh (4,20)], although transmission quality can be guaranteed even if N_u exceeds 40, its transmission rate only reaches 125 Mbps. In this situation, if the number of users is fewer, the rate resource is wasted. Comparatively, according to N_u , AMAM can choose the best resource distribution scheme adaptively and adjust the value of R_b . In this way, on the premise of a reliable communication system, resources can be fully utilized. The disadvantage of uneven resource distribution of FMAM is overcome and the transmission rate is higher than that of FMAM.

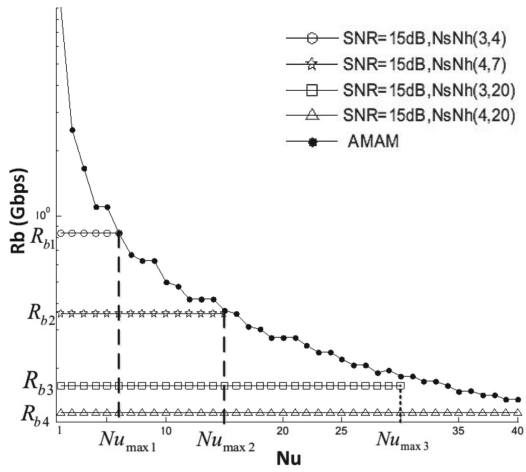


Fig. 4. Relationship between N_u and R_b under AMAM and FMAM

4.2 Relationship Between N_u and P_{ave} Average Power

The value of average power P_{ave} reflects the power consumption level of an intra/inter-chip wireless interconnection system. Figure 5 shows the relationship between N_u and P_{ave} under the schemes of AMAM and FMAM separately. In Fig. 5, each FMAM corresponds to a fixed P_{ave} and when the SNR of each pulse is certain, the value of P_{ave} is proportional to the number of pulse N_s . For example, for FMAM with the same rate, such as [SNR = 15 dB, $N_s N_h(3,8)$] and [SNR = 15 dB, $N_s N_h(8,3)$], the P_{ave} that the former corresponds to is smaller than the P_{ave} that the latter corresponds to. In addition, as described in Sect. 4.1, each FMAM also corresponds to one $N_{u_{max i}}$, which indicates the maximum number of users supported by the communication system with reliable quality. For example, when SNR = 15 dB, the schemes of $N_s N_h(3,8)$, $N_s N_h(8,3)$, $N_s N_h(12,3)$, and $N_s N_h(20,3)$ that correspond to the values of $N_{u_{max i}}$ are 12, 14, 21, and 35 separately. However, the disadvantages of FMAM are that only if $N_u = N_{u_{max i}}$ can the system resource be fully used; if $N_u < N_{u_{max i}}$, then a large amount of system resource is wasted; if $N_u > N_{u_{max i}}$, system reliability is not guaranteed. In the AMAM scheme, the power P can be adjusted timely according to the number of users in the system, that is, the reduction of N_u decreases the power while the increment of N_u properly raises the power to resist MUI. AMAM keeps the system relatively stable and, compared with FMAM, it has a higher utilization rate of energy.

Although the AMAM scheme raises the complexity of chip design to a certain extent, with the constant increase of hardware design level, its relatively higher complexity does not impede its development. AMAM has obvious advantages in rate and power resource distribution, and it can utilize maximum system resource and relieve random noise interference caused by random change of user access. As a result, AMAM is highly applicable and indispensable to WCAN.

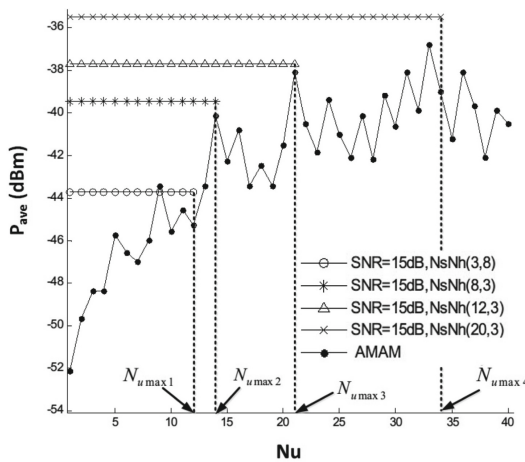


Fig. 5. Relationship between N_u and P_{ave} under AMAM and FMAM

5 Conclusion

Intra/inter-chip wireless interconnection technology complements the smart grid system to compensate for the shortcomings of traditional grid operation modes. With the promotion of 5G technologies, WCAN is becoming one of the applications of the 5G ultra dense network. To solve the problem of multi-user network communication in WCAN, the multi-user interference characteristics of WCAN under TH-PPM multiple-access modulation are analyzed, and the system BER performance analytical model is proposed. Based on this model and by weighing communication quality, rate, and power consumption, the adaptive multiple-access scheme applicable to WCAN is designed. Performance simulation and analysis show that this scheme can guarantee the reliability of intra/inter-chip interconnection, allocate system resources appropriately, and elevate system capacity and transmission performance effectively. At the same time, this scheme reduces realization complexity and power consumption. The results provide a reference for multi-user communication and large capacity in the smart grid system.

Acknowledgment. This study was supported by the Beijing Natural Science Foundation - Foundation of Municipal Commission of Education (KZ201911232046), the Beijing Natural Science Foundation - Haidian Original Innovation Joint Fund Focused on Special Projects (L182039), and the Beijing Natural Science Foundation - Haidian Primitive Innovation Joint Fund Frontier Project (L182032). The authors declare no conflict of interest.

References

1. Dragičević, T., Siano, P., Prabakaran, S.R.: Future generation 5G wireless networks for smart grid: a comprehensive review. *Energies* **12**(11), 2140 (2019)
2. Ma, K., Liu, X., Liu, Z., et al.: Cooperative relaying strategies for smart grid communications: bargaining models and solutions. *IEEE Internet Things J.* **4**(6), 2315–2325 (2017)
3. Akpakwu, G.A., Silva, B.J., Hancke, G.P., et al.: A survey on 5G networks for the Internet of Things: communication technologies and challenges. *IEEE Access* **6**, 3619–3647 (2017)
4. Foulon, S., Pruvost, S., Loyez, C., et al.: A 10Gbits/s 2.1pJ/bit OOK demodulator at 60GHz for chip-to-chip wireless communication. In: 2012 IEEE Radio and Wireless Symposium (RWS), Santa Clara, CA, pp. 291–294 (2012)
5. Afroz, S., Amir, M.F., Saha, A., et al.: A 10Gbps UWB transmitter for wireless inter-chip and intra-chip communication. In: 2010 International Conference on Electrical and Computer Engineering (ICECE), pp. 104–107 (2010)
6. Kubota, S., Toya, A., Sugitani, T., et al.: 5-Gb/s and 10-GHz center-frequency Gaussian monocycle pulse transmission using 65-nm logic CMOS with on-chip dipole antenna and high- κ interposer. *IEEE Trans. Compon. Packag. Manuf. Technol.* **4**(7), 1193–1200 (2014)
7. Wang, G., Xiang, W., Yuan, J.: Outage performance for compute-and-forward in generalized multi-way relay channels. *IEEE Commun. Lett.* **16**(12), 2099–2102 (2012)

8. Peng, Y., et al.: Secret key generation based on estimated channel state information for TDD-OFDM systems over fading channels. *IEEE Trans. Wirel. Commun.* **16**(8), 5176–5186 (2017)
9. Yeh, H.H.: Developments of 60 GHz antenna and wireless interconnect inside multi-chip module for parallel processor system. University of Arizona, Tucson, AZ (2013)
10. Karim, M.R., Yang, X., Shafique, M.F.: On chip antenna measurement: a survey of challenges and recent trends. *IEEE Access* **6**, 20320–20333 (2018)
11. Gimeno, C., Flandre, D., Bol, D.: Analysis and specification of an IR-UWB transceiver for high-speed chip-to-chip communication in a server chassis. *IEEE Trans. Circuits Syst. I Regul. Pap.* **65**(6), 2015–2023 (2017)
12. Catania, V., Mineo, A., Monteleone, S., et al.: Improving energy efficiency in wireless network-on-chip architectures[J]. *ACM Journal on Emerging Technologies in Computing Systems (JETC)* **14**(1) (2018). Article No. 9
13. Bidwai, S.S., Bidwai, S.S., Mandrupkar, S.G.: Wireless NoC-a revolutionary alternative as interconnection fabric. In: 2018 3rd International Conference for Convergence in Technology (I2CT), pp. 1–4. *IEEE* (2018)
14. Vijayakumaran, V., Yuvaraj, M.P., Mansoor, N., et al.: CDMA enabled wireless network-on-chip. *ACM J. Emerg. Technol. Comput. Syst. (JETC)* **10**(4) (2014). Article No. 28
15. Raju, S., Salahuddin, S.M., Islam, M.S., et al.: DSSS IR UWB transceiver for intra/inter chip wireless interconnect in future ULSI using reconfigurable mono-cycle pulse. In: 2008 International Conference on Computer and Communication Engineering, ICCCE 2008, pp. 306–309. *IEEE* (2008)
16. Saha, P.K., Sasaki, N., Kikkawa, T.: A CMOS UWB transmitter for intra/inter-chip wireless communication. In: 2004 IEEE Eighth International Symposium on Spread Spectrum Techniques & Applications, Australia, pp. 962–966 (2004)
17. He, J., Zhang, Y.P.: A CMOS ultra-wideband impulse radio transceiver for inter-chip wireless communications. In: 2007 IEEE International Conference on Ultra-Wideband, Singapore, pp. 626–631 (2007)
18. Kim, K.: Design and characterization of RF components for inter and intra-chip wireless communications. Ph.D dissertation, Gainesville, University of Florida, FL (2000)
19. Scholtz, R.A.: Multiple access with time-hopping impulse modulation. In: Military Communications Conference, Boston, MA, pp. 447–450 (1993)
20. Long, H., et al.: Secrecy capacity enhancement with distributed precoding in multirelay wiretap systems. *IEEE Trans. Inf. Forensics Secur.* **8**(1), 229–238 (2012)
21. Qiu, H.B., Zheng, L.: New method of BER calculate for impulse-UWB TH-PPM multiple-access communications. *J. Commun.* **10**, 133–137 (2005)
22. Le Boudec, J.Y., Merz, R., Radunovic, B., et al.: A MAC protocol for UWB very low power mobile ad-hoc networks based on dynamic channel coding with interference mitigation (2004)
23. Biradar, G.S., Merchant, S.N., Desai, U.B.: An adaptive frequency and time hopping PPM UWB for multiple access communication. In: 2007 6th International Conference on Information, Communications & Signal Processing, pp. 1–5. *IEEE* (2007)